Please cite this article as:
Bohdan Mochnacki, Sylwia Lara, Edyta Pawlak, Application of the enthalpy approach in numerical modelling of solidification process, Scientific Research of the Institute of Mathematics and Computer Science, 2002, Volume 1, Issue 1, pages 163-176.
The website: http://www.amcm.pcz.pl/
Prace Naukowe Instytutu Matematyki i Informatyki Politechniki Częstochowskiej

APPLICATION OF THE ENTHALPY APPROACH IN NUMERICAL MODELLING OF SOLIDIFICATION PROCESS

Bohdan Mochnacki, Sylwia Lara, Edyta Pawlak

Institute of Mathematics and Computer Science, Technical University of Częstochowa

Abstract. The numerical modelling of the Stefan problem using directly the typical description of the process is rather difficult. In this connection one can find in literature the models basing on the enthalpy convention and the artificial mushy zone introduction. This paper summarizes the state of the art of the enthalpy models of phase change problems. The part of the approaches discussed has been modified by the authors of the paper, we also present the new interpretations of some models.

1. The Stefan problem

We consider the solidification of pure metals. The typical feature of the process discussed is the constant temperature T^* of phase change. The transient temperature field in non-homogeneous domain of solidifying metal is described by the system of partial differential equations:

$$c_e \partial_t T_e(x,T) = \nabla\left[\lambda_e \nabla T_e(x,T)\right] \tag{1}$$

where e = 1, 2 corresponds to the solid and liquid sub-domains, c_e [J/m^3 K] is the volumetric specific heat, λ_e [W/mK] is the thermal conductivity. On the moving boundary Γ_{12} between sub-domains we have the continuity condition in the form

$$\begin{cases} -\lambda_2 \partial_n T_2(x,\ T) = -\lambda_1 \partial_n T_1(x,\ T) + v_n L \\ T_2(x,\ T) = T_1(x,\ T) = T^* \end{cases} \tag{2}$$

called in literature the Stefan condition. Here $\partial_n T$ is the normal derivative at the boundary point, v_n is the solidification rate in the normal direction, L [J/m^3] is the volumetric latent heat. On the outer surface Γ_0 of the system the boundary condition in general form

$$\Phi\left[T(x,\ T) = \partial_n T(x,\ T)\right] = 0 \tag{3}$$

is given. For time t = 0 the initial distribution of temperature is known.
From the numerical point of view the model above model is not very convenient and in the next chapters the others approaches to the Stefan problem description will be presented.

2. Temperature recovery method

We introduce to the consideration the physical enthalpy of metal defined as follows

$$H(T) = \int_{T_r}^{T} c(\mu)\, d\mu + \eta(T)\, L \tag{4}$$

where for $T > T^*$: $c(T) = c_2$ and for $T < T^*$: $c(T) = c_1$, while

$$\eta(T) = \begin{cases} 0 & T < T^* \\ 1 & T \geq T^* \end{cases} \tag{5}$$

The course of enthalpy function is shown in Figure 1.

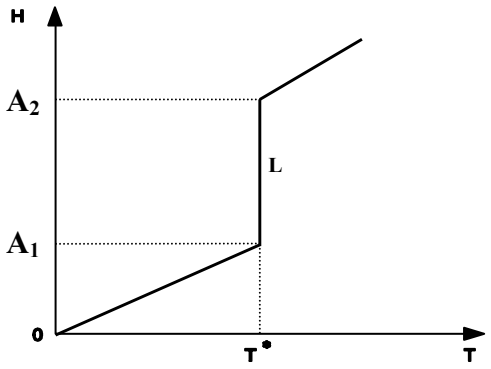

Fig. 1. Enthalpy-temperature function

Using the definition (4) one can transform the energy equations to the form

$$\partial_t H(x,T) = \nabla\left[\lambda \nabla T(x,T)\right] \tag{6}$$

It should be pointed out that for such mixed enthalpy-temperature convention the formulation of the Stefan condition is needless from the computational view point. If we use the typical numerical algorithm in which the domain is covered by the mesh (e.g. FDM, FEM, BEM, collocational methods), then if the enthalpy at the node considered x_i, $i = 1,2,...N$, is from the range $[A_1,A_2]$ then the temperature $T(x_i,t)$ at this point equals T^*. This value is accepted until $H(x_i,t) < A_1$.

The idea of the temperature recovery method (TRM) is practically the same, but we consider only temperature formulation (it is more convenient on the stage of the numerical algorithm construction). So we introduce the quantity of local temperature reserve z_i defined as follows [1]

$$z_i = z(x_i, t) = \frac{L}{c_2} \tag{7}$$

Using the numerical methods we find the temperatures T_i^f at nodes X_i for successive times t^f, $f = 0,1,...F$. If at the moment t^f temperature T_i^f drops below T^* then we accept at this point the temperature T^*, while the temperature reserve is decreased, namely

$$z_i \to z_i - \left(T^* - T_i^f\right) \tag{8}$$

The same procedure is repeated in successive loops. If for the node x_i $z_i < 0$ we accept $z_i = 0$ and next computations are realized without the temperature correction. The physical interpretation of TRM is the following (see Fig. 2).

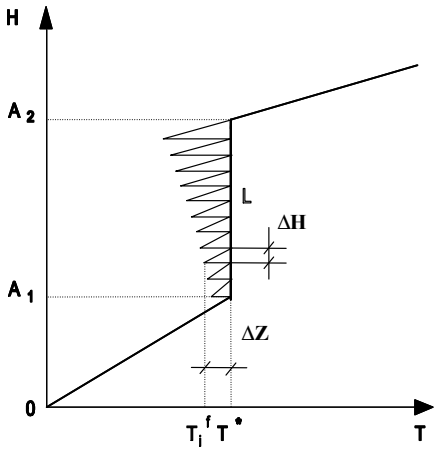

Fig. 2. Interpretation of TRM

The change of unitary enthalpy corresponding to the change of temperature from T^* to T_i^f found under the assumption that we consider the cooling of molten metal equals

$$\Delta H_i = c_2\left(T^* - T_i^f\right) \tag{9}$$

This value we treat as the partial exhaustion' of latent heat L, in particular

$$L \to L - \left(T^* - T_i^f\right) \tag{10}$$

Dividing the last formula by c_2 we obtain

$$\frac{L}{c_2} \to \frac{L}{c_2} - \left(T^* - T_i^f\right) \tag{11}$$

The similar approach can be used in the case of solidification in the temperature interval [2-4].

3. Alternating phase truncation method

The first version of the method has been presented by Rogers, Berger and Ciment in [5, 6]. Next it was generalized by Majchrzak, Mochnacki and Kapusta [7, 8]. The essence of the method is the artificial homogenization of the domain considered. The computations concerning the transition from moment t to moment $t + \Delta t$ are realized in two stages corresponding to the parameters of molten metal and solid state (we present the basic version of APTM concerning the Stefan problem). The mathematical description of the solidification process we formulate using the enthalpy convention. So, we consider the system of equations

$$\partial_t H_e(x, T) = \nabla\left[a_e \nabla H_e(x, T)\right] \tag{12}$$

where a_e is the diffusion coefficient. This system is supplemented by the boundary--initial conditions

$$\left.\begin{array}{ll} x \in \Gamma_{1,2}(t): & \left\{\begin{array}{c} -a_2 \partial_n H_2(x, T) = -a_1 \partial_n H_1(x, T) + L v_n \\ A_2 = A_1 + L \end{array}\right. \\ x \in \Gamma_0: & \Phi\left[H,\ \partial_n H(x,T)\right] = 0 \\ t = 0: & H_e(x,0) = H_{e0}(x), \quad e = 1,\ 2 \end{array}\right\} \tag{13}$$

The APTM algorithm for the transition from $t = t^{f-1}$ to $t + \Delta t = t^f$ is the following.
Let us denote by H_i^{f-1} the discrete set of enthalpy values in the domain of metal at time t^{f-1}.
In the first stage of computation the domain considered is conventionally reduced to the liquid state. It corresponds to the assumption of the pseudo-initial condition in the form

$$V_1(x_i, t^{f-1}) = \max\left\{H_i^{f-1}, A_2\right\} \tag{14}$$

Next using the optional numerical method we find the solution for time t^f, this means $V_1'(x_i, t^f)$ (the diffusion coefficient is assumed to be $a = a_2$). Now we correct the obtained solution, namely

$$V_1(x_i, t^f) = V_1'(x_i, t^f) + H_i^{f-1} - V_1(x_i, t^{f-1}) \tag{15}$$

The second stage starts from the formulation of the new pseudo-initial condition for transition $t^{f-1} \to t^f$

$$V_2(x_i,\ t^{f-1}) \ =\ \min\left\{A_1, V_1(x_i, t^f)\right\} \tag{16}$$

It corresponds to the conventional reduction of metal domain to the solid phase. We find the enthalpy field $V_2'(X_i,\ t^f)$ (assuming $a = a_1$) and we correct the result obtained using the formula

$$H_i^f = V_2'(x_i, t^f) \ +\ V_1(x_i, t^f) \ -\ V_2(x_i, t^{f-1}) \tag{17}$$

In Figures 3 and 4 the successive stages of computations are shown.

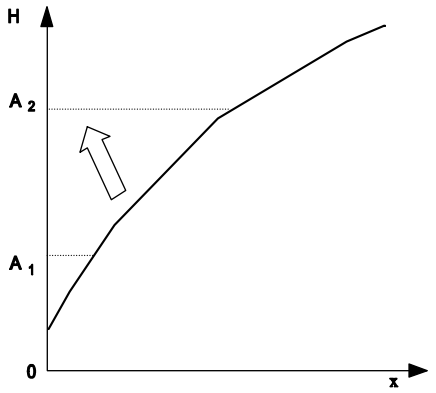

Fig. 3. Condition $V_1(x_i, t^{f-1})$

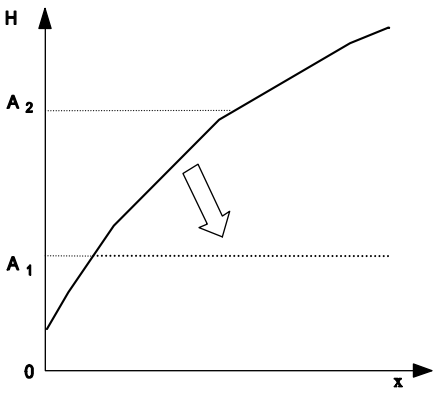

Fig. 4. Condition $V_2(x_i, t^{f-1})$

The correctness of the algorithm discussed is proved in [6].

4. The Hsiao method [9]

The method presented bases on the artificial mushy zone (AMZ) introduction. The solidification point is substituted by a temperature interval $[T^- = T^* - \Delta T,\ T^+ = T^* + \Delta]$.

The real enthalpy-temperature diagram is transformed to the form shown in Figure 5. In this way one can define the substitute thermal capacity of AMZ sub-domain (the slope of the sector between $T^* - \Delta T$ and $T^* + \Delta T$).

So

$$T \in \left[T^-, T^+\right]: \quad c_{1,2} = \frac{L}{T^+ - T^-} = \frac{L}{2\Delta T} \tag{18}$$

If we assume the constant values of c_1 and c_2 then the thermal capacity of the metal is determined by the piece-vise function

$$c(T)=\begin{cases} c_2 & T > T^+ \\ c_{12} & T^- \le T \le T^+ \\ c_1 & T < T^- \end{cases} \tag{19}$$

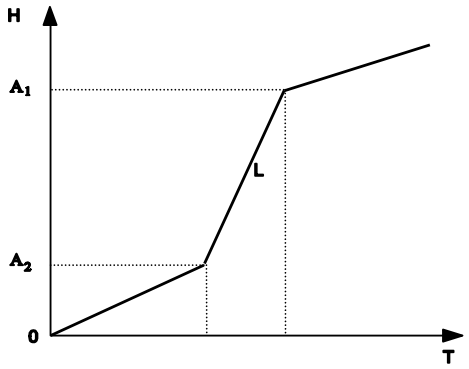

Fig. 5. Artificial mushy zone

The course of function $c(T)$ is shown in Figure 6.

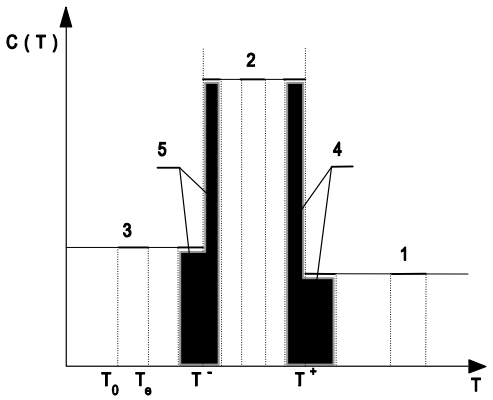

Fig. 6. Thermal capacity of metal

Let us denote by 0 and k two adjoining points resulting from the domain disretization (node 0 is a central point). We define the thermal capacity c_{0k} in the following way:

$$c_{0k} = \frac{1}{T_k - T_0} \int_{T_0}^{T_k} c(T)\, dT \tag{20}$$

and we obtain

$$
\begin{aligned}
&T_0,\, T_k > T^+: && c_{0k} = c_2 \\
&T_0,\, T_k \in \left[T^-,\, T^+\right]: && c_{0k} = c_{12} \\
&T_0,\, T_k < T^-: && c_{0k} = c_1 \\
&T_0 \in \left[T^-,\, T^+\right],\quad T_k > T^+: && c_{0k} = \frac{c_2\left(T_k - T^+\right) + c_{12}\left(T^+ - T_0\right)}{T_k - T_0} \\
&T_0 < T^-,\quad T_k \in \left[T^-,\, T^+\right]: && c_{0k} = \frac{c_{12}\left(T_k - T^-\right) + c_1\left(T^- - T_0\right)}{T_k - T_0} \\
&T_k > T^+,\quad T_0 < T^-: && c_{0k} = \frac{c_2\left(T_k - T^+\right) + c_{12}\left(T^+ - T^-\right) + c_1\left(T^- - T_0\right)}{T_k - T_0}
\end{aligned}
\tag{21}
$$

The similar formulas can be found for the case $T_k < T_0$.
Let $k = 1,2,...,n$ denote indexes of the all adjoining nodes of node 0. Then we define the thermal capacity at the central node as

$$c_0 = \sum_{k=1}^{n} c_{0k} w_k \tag{22}$$

where

$$w_k = \frac{\rho_k}{\sum_{k=1}^{n} \rho_k} \tag{23}$$

at the same time ρ_k is the distance between points 0 and k. The numerical experiments done by Hsiao and also verified by the authors of above paper show that such approach gives quite good solution of the Stefan problem and the value of interval assumed $[T^-, T^+]$ is not very essential.
In the version presented by Hsiao the numerical algorithm of solidification problem solution is rather complicated. In the paper [10] we present its modification and we show that the definition of c_{0k} results from the following considerations.
Because

$$\int_{T_0}^{T_k} c(T)\, dT = \int_{0}^{T_k} c(T)\, dT - \int_{0}^{T_0} c(T)\, dT \tag{24}$$

and next

$$\int_0^{T_k} c(T)\,dT - \int_0^{T_0} c(T)\,dT = H(T_k) - H(T_0) \tag{25}$$

Finally

$$c_{0k} = \frac{H(T_k) - H(T_0)}{T_k - T_0} \tag{26}$$

at the same time the relation $T_e > T_0$ or $T_e < T_0$ is here not essential. The interpretation of formula (26) is shown in Figure 7.

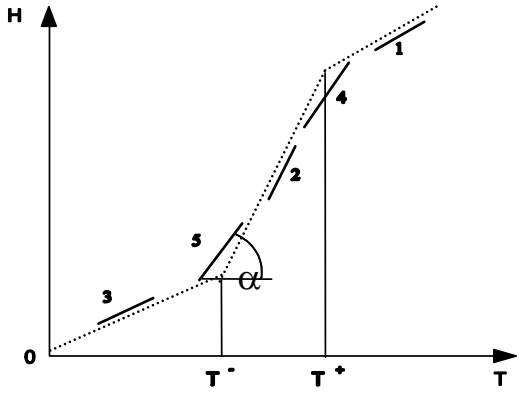

Fig. 7. Thermal capacity c_{0k}

5. Application of the Kirchhoff function

The Kirchhoff function (Kirchhoff's transformation) linearizes the Laplace or Poisson equation in which the thermal conductivity is temperature-dependent.
The Kirchhoff function is defined as follows

$$U(T) = \int_{T_r}^{T} \lambda(\mu)\,d\mu \tag{27}$$

where T_r is a reference level.
If we consider the Stefan problem using the artificial mushy zone approach then the energy equation in which the Kirchhoff function is introduces takes a form

$$\partial_t H(x, T) = \nabla\left[\nabla U(x, T)\right] \tag{28}$$

The functions $H = H(T)$ and $U = U(T)$ are monotonic ones and we can find the dependence $H = \Psi(U)$. Because

$$\frac{\partial H(x,t)}{\partial t} = \frac{d H(U)}{dU}\frac{\partial U(x,t)}{\partial t} = \Psi'(U)\frac{\partial U(x,t)}{\partial t} \tag{29}$$

therefore the energy equation can be written in the form

$$\Psi'(U)\frac{\partial U(x,t)}{\partial t} = \nabla\left[\nabla U(x, T)\right] \tag{30}$$

The function $\Psi(U)$ and its derivative one can determine on the basis of the experimental data using the numerical methods. The knowledge of courses of the enthalpy $H(T)$ and Kirchhoff's transformation $U(T)$ allows to construct the function $\Psi(U)$ - Fig. 8.

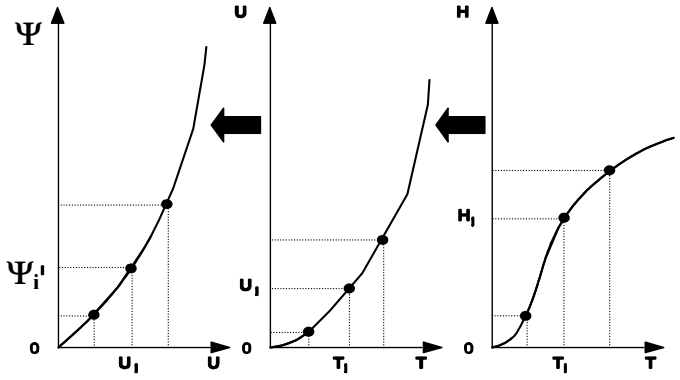

Fig. 8. Construction of $\Psi(U)$

Such approach requires, of course, the formulation of the boundary and initial conditions using the Kirchhoff function [11].

6. The generalized Stefan problem

We will consider the metal for which the solidification process proceeds partially at the constant temperature and partially in the interval of temperatures. Such situation takes place, among others in the case of cast iron solidification (Fig. 9).

The example of the course of enthalpy function for generalized Stefan problem is shown in Figure 10.

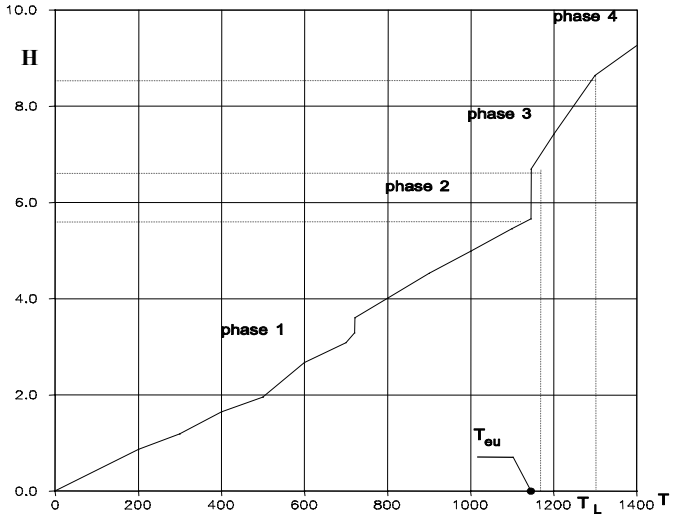

Fig. 9. Enthalpy diagram (cast iron CE = 3.95)

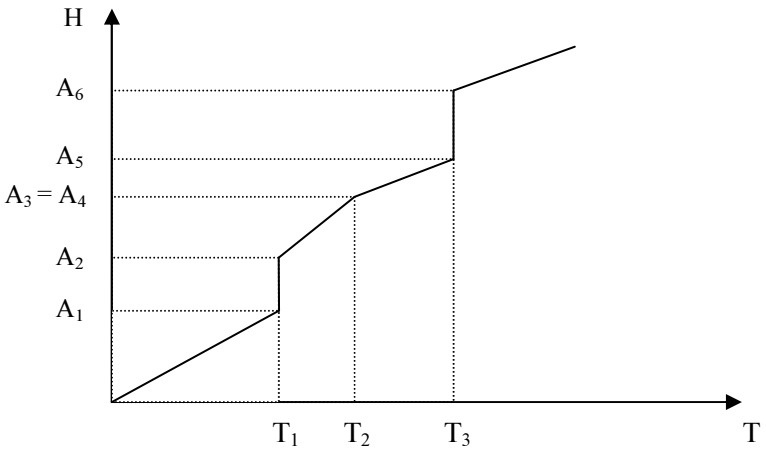

Fig. 10. Generalized course of enthalpy

In such case the function H(T) is determined by the formula

$$H(T)=\begin{cases} A_0 + c_1(T-T_0) & T < T_1 \\ A_2 + c_2(T-T_1) & T_1 \le T < T_2 \\ \vdots & \\ A_{2n-2} + c_n(T-T_{n-1}) & T_{n-1} \le T < T_n \end{cases} \tag{31}$$

We can find the inverse function, namely (see Fig. 11):

$$T(H)=\begin{cases} T_0+\dfrac{H-A_0}{c_1} & H<A_1 \\ T_1 & A_1\le H<A_2 \\ T_1+\dfrac{H-A_2}{c_2} & A_2\le H<A_3 \\ \vdots & \\ T_{n-1} & A_{2n-3}\le H<A_{2n-2} \\ T_{n-1}+\dfrac{H-A_{2n-2}}{c_n} & A_{2n-2}\le H<A_{2n-1} \end{cases} \tag{32}$$

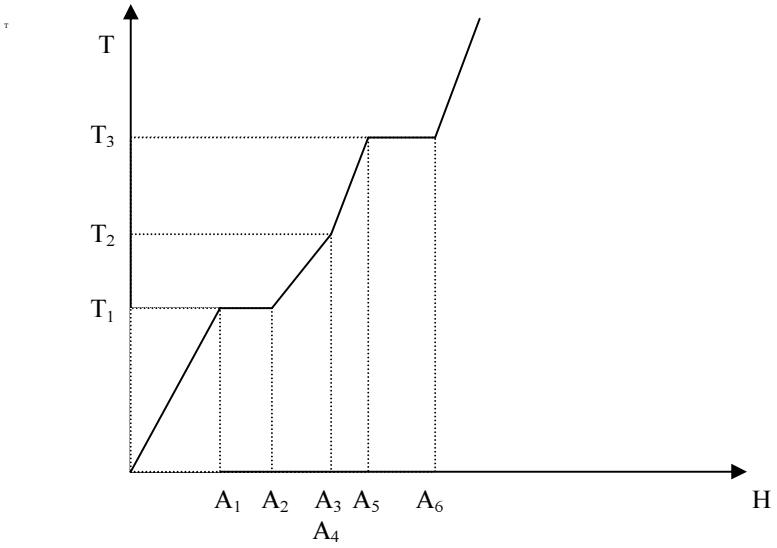

Fig. 11. The inverse function

Now we introduce the Kirchhoff transformation defined as follows (Fig. 12)

$$U(T)=\begin{cases} B_0+\lambda_1(T-T_0) & T<T_1 \\ B_1+\lambda_2(T-T_1) & T_1\le T<T_2 \\ \vdots & \\ B_{n-1}+\lambda_n(T-T_{n-1}) & T_{n-1}\le T<T_n \end{cases} \tag{33}$$

where:

$$\begin{aligned} B_0 &= 0 \\ B_1 &= \lambda_1 T_1 = B_0 + \lambda_1 (T_1 - T_0) \\ B_2 &= B_1 + \lambda_2 (T_2 - T_1) \\ &\vdots \\ B_{n-1} &= B_{n-2} + \lambda_{n-1} (T_{n-1} - T_{n-2}) \end{aligned} \tag{34}$$

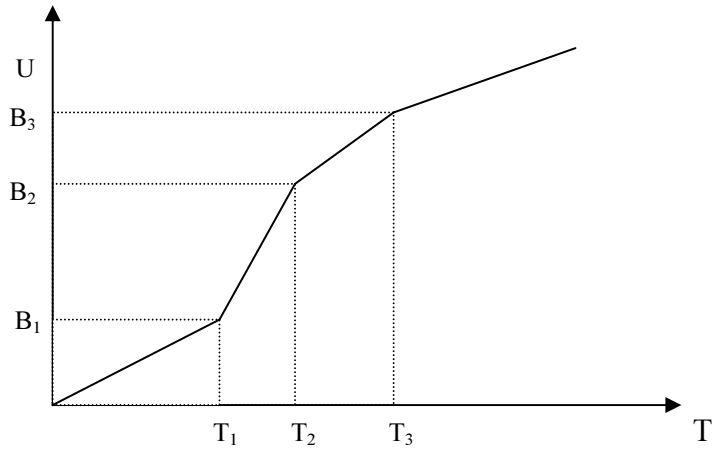

Fig. 12. The Kirchhoff function

Finally we can construct the dependence between U and H (Fig. 13) in the form

$$U(H) = \begin{cases} B_0 + a_1 (H - A_0) & H < A_1 \\ B_1 & A_1 \le H < A_2 \\ B_1 + a_2 (H - A_2) & A_2 \le H < A_3 \\ \vdots & \\ B_{n-1} & A_{2n-3} \le H < A_{2n-2} \\ B_{n-1} + a_n (H - A_{2n-2}) & A_{2n-2} \le H < A_{2n-1} \end{cases} \tag{35}$$

where

$$a_i = \frac{\lambda_i}{c_i} \qquad i = 1,2,...,n \tag{36}$$

The course of function *U(H)* corresponding to the previous figure shown in Figure 13. So, the energy equation written in the enthalpy convention is the following

$$\frac{\partial H(x,t)}{\partial t} = div\{grad[A(H)H + B(H)]\} \tag{37}$$

where:

$$A(H) = \begin{cases} a_1 \\ 0 \\ a_2 \\ \vdots \\ 0 \\ a_n \end{cases} \qquad B(H) = \begin{cases} B_0 - a_1 A_0 \\ B \\ B_1 - a_2 A_2 \\ \vdots \\ B_{n-1} \\ B_{n-1} - a_n A_{2n-2} \end{cases} \tag{38}$$

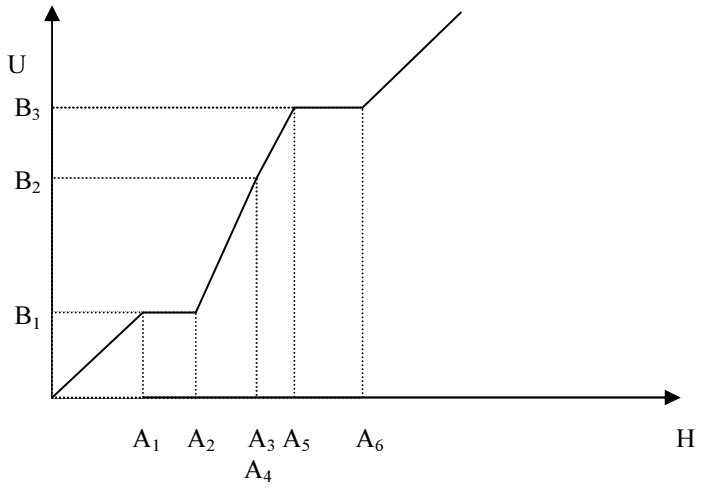

Fig. 13. The dependence between U and H

Presented in this paper approach is very convenient for numerical simulation of solidification process both in the case of classical Stefan problem and also for the generalized one.

References

[1] Hong C.P., Umeda T., Kimura Y., Numerical models for casting solidification problems, Metal. Trans. 1984, 15B, 101-105.

[2] Mochnacki B., Szopa R., Application of the BEM in numerical modelling of solidification, Part 1, J. of Theor. and Appl. Mech. 1998, 2, 36, 457-468.

[3] Majchrzak E., Mochnacki B., The BEM application for numerical solution of non-steady and non-linear thermal diffusion problems, CAMES 1996, 2, 4, 327-346.

[4] Szopa R., Modelowanie krzepnięcia i krystalizacji z wykorzystaniem kombinowanej metody elementów brzegowych, ZN Pol. Śl. 1999, Hutnictwo 54.

[5] Rogers J., Berger A., Ciment M., Numerical solution of a diffusion consumption problem with free boundary, SIAM J. Num. Anal. 1975, 12, 645-659.

[6] Rogers J., Berger A., Ciment M., The alternating phase truncation method for a Stefan problem, SIAM J. Num. Anal. 1979, 16, 562-587.

[7] Mochnacki B., Suchy J., Numerical modelling of casting solidification, The concept of problem linearization, ASF Transactions 1997, 96-11, 203-209.

[8] Mochnacki B., Majchrzak E., Suchy J.S., Thermal theory of foundry processes - a base of numerical simulation of casting solidification - chapter 2, 31-66 (in:) Casting Simulation. Background and Examples, World Foundrymen Organization, International Commission 3.3: „Computer Simulation of Casting Processes".

[9] Hsiao J.S., An efficient algorithm for finite-difference analyses of heat transfer with melting and solidification, Numerical Heat Transfer 1985, 8, 653-666.

[10] Mochnacki B., Lara S., Pawlak E., Numerical solution of 2D Stefan problem, Solidification of Metals and Alloys 2000, 2, 44, 235-238.

[11] Cao Y., Fagri A., Chang W.E., Numerical analysis of Stefan problem, Int. J. of Heat and Mass Transfer 1989, 32, 7, 1289-1298.